

Onset of Topological Constraints in Polymer Melts: A Mode Analysis by Neutron Spin Echo Spectroscopy

D. Richter, L. Willner, and A. Zirkel

Institut für Festkörperforschung, Forschungszentrum Jülich, 52425 Jülich, Germany

B. Farago

Institut Laue-Langevin, 38042 Grenoble, France

and Laboratoire Léon Brillouin (Laboratoire Commune, Commissariat à l'Energie Atomique/Centre National de la Recherche Scientifique), Saclay, France

L. J. Fetters and J. S. Huang

Exxon Research and Engineering Corporation, Annandale, New Jersey 08801

(Received 17 September 1993)

By neutron spin echo spectroscopy we have investigated the dynamic structure factors for single chain relaxation in polymer melts varying the molecular weight through the transition from unrestricted Rouse motion to entanglement controlled behavior. From an analysis of the structure factors with respect to the different relaxation modes we found that, depending on their spatial extension in relation to the entanglement length, large-scale relaxations are successively suppressed with increasing molecular weight. A comparison with macroscopic diffusion and viscosity data yields excellent internal consistency.

PACS numbers: 61.25.Hq, 61.12.Ex

Over an extended time interval dense long chain polymer liquids respond elastically like rubbers to external strain. Guided by the analogy to the rubbery response which originates from the entropy elasticity of polymeric strands between permanent cross links, the elastic properties of polymer melts are explained via the conjecture of the existence of a temporary network formed by chain entanglements [1]. In the reptation theory these constraints are modeled in terms of a tube of a width given by the entanglement distance d following the coarse grained chain profile. Chain motion is then restricted to the tube which can only be left by its ends [2]. Though the entanglement distance is of crucial importance for the understanding of polymer viscoelasticity, only recently has this length been observed directly on a microscopic scale by neutron spin echo (NSE) [3,4].

In order for entanglement constraints to become active, the polymer chains have to exceed a critical molecular weight M_c corresponding roughly to 2.5 times the size of the entanglement strand M_e in the entangled melt [1]. In this Letter we report on an investigation of the dynamic structure factor from single protonated polyethylene (PE) chains in deuterated PE melts varying the molecular weight through this critical range using neutron spin echo spectroscopy. As a function of momentum transfer $Q = 4\pi/\lambda \sin\vartheta$ (λ : neutron wavelength, 2ϑ : scattering angle) the different chain relaxation modes contribute to the dynamic structure factor in a distinct way. Exploiting this Q dependence for the first time it has become possible to analyze separately the relaxation behavior of the different large-scale relaxation modes in polymer melts. With increasing molecular weight we find a successive slowing down at the first modes. The relaxation times are stretched particularly if the spatial extent of a mode exceeds a distance corresponding to the entanglement

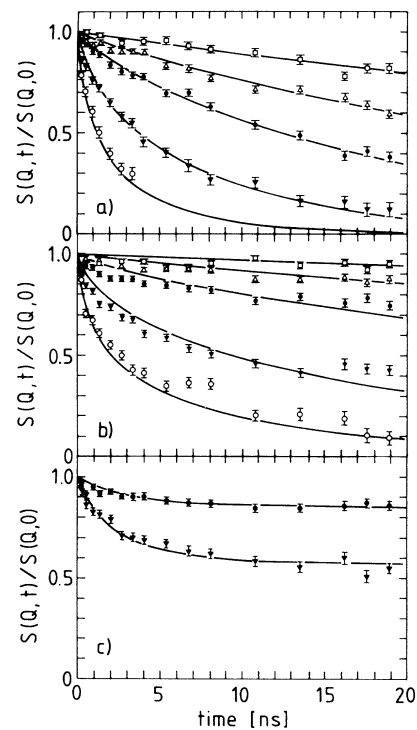


FIG. 1. Dynamic structure factors for PEB-2 polymer melts of different molecular weights: (a) $M_w = 2.0 \times 10^3$, (b) $M_w = 4.8 \times 10^3$, and (c) $M_w = 36.0 \times 10^3$. For (a) and (b) the Q values are from above: $Q = 0.037, 0.055, 0.077, 0.115, \text{ and } 0.155 \text{ \AA}^{-1}$. The two spectra displayed in (c) correspond to $Q = 0.077$ and $Q = 0.115 \text{ \AA}^{-1}$. The solid lines in (a) and (b) display the result of the mode analysis (see text); in (c) they represent a fit with the asymptotic Ronca model [4,8]. For the purpose of this paper they may be taken as guide lines for the eye.

mesh in the long chain melt. Diffusion coefficients and viscosities evaluated from the dynamic structure factors agree well with macroscopic results on the same polymer.

The polyethylene samples were prepared via saturation of polybutadiene precursor polymers, which were synthesized via standard anionic polymerization techniques. Size exclusion chromatography was used to evaluate the molecular weights M_w and heterogeneity indices M_w/M_n . The polydienes were saturated by hydrogen or deuterium, respectively, yielding polyethylene-1 butene copolymer, which is designated as PEB-2, where the integer denotes the approximate number of ethyl branches per 100 backbone atoms. Because of the small fraction of less than 1 ethyl branch per 50 monomers it essentially resembles polyethylene. The following samples were studied: PE 2000: $M_w = 2 \times 10^3$; PE 3600: $M_w = 3.6 \times 10^3$; PE 4800: $M_w = 4.8 \times 10^3$; PE 6500: $M_w = 6.5 \times 10^3$; and PE 36000: $M_w = 36 \times 10^3$. The heterogeneity indices were in the range $1.07 \geq M_w/M_n \geq 1.02$. In order to investigate the intrachain coherent structure factor 15% labeled protonated chains of corresponding molecular weights were blended to each deuterated specimen.

The neutron scattering experiments were carried out at the neutron spin echo spectrometer at the Orphée-Reactor in Saclay. In order to relate to earlier experiments on high molecular weight PEB-2 chains [4], the

experiment was performed at 509 K. Standard background and resolution corrections were undertaken.

An NSE experiment on a coherently scattered sample measures directly the normalized dynamic structure factor $S(Q,t)/S(Q,0)$ [5]. Figure 1 presents representative results from the PE 2000 and PE 4800 samples together with those observed on the long chain PE 36000 sample. Obviously the dynamic structure factors for short chains decay much more rapidly than those for long chains. Furthermore, no indication of a plateau in the relaxation function at long times signifying an entanglement mesh is visible. We note that in going from $M_w = 2.0 \times 10^3$ to $M_w = 4.8 \times 10^3$, the spectral decay is already considerably reduced. For example, at $Q = 0.115 \text{ \AA}^{-1}$ the spectrum from PE 2000 decays to about 0.1, while that from PE 4800 only decays to about 0.4. Thus it appears that at higher molecular weight considerable constraints on the chain relaxation are already exerted.

In order to analyze the observed spectra in a more quantitative way, one cannot resort to the asymptotic scattering functions available for the Rouse model [6,7] or for entanglement controlled behavior [8]. For short chains the detailed mode structure of the relaxing chain becomes important. For a random Gaussian chain [9], for which the relaxation behavior can be described in terms of Rouse modes, the dynamic structure factor has the general form [2]

$$S(Q,t) = \frac{1}{N} \exp \left[-\frac{Q^2}{6} \langle [x_0(t) - x_0(0)]^2 \rangle \right] \times \left\{ \sum_{m,n} \exp \left[-\frac{1}{6} Q^2 l^2 |m-n| - \frac{4R_g^2 Q^2}{\pi^2} \sum_{p=1}^N \frac{1}{p^2} \cos \left[\frac{p\pi m}{N} \right] \cos \left[\frac{p\pi n}{N} \right] [1 - \langle x_p(t)x_p(0) \rangle] \right] \right\}. \quad (1)$$

Thereby x_0 describes the center of mass coordinates, x_p is the normal coordinate of mode p , R_g the radius of gyration, N the number of chain segments, and l the segment length ($l^2 = C_\infty l_0^2 = 13.76 \text{ \AA}^2$; l_0 : bond length; C_∞ : characteristic ratio [10]). In the case of unrestricted Rouse motion the normalized correlators read

$$\langle x_p(t)x_p(0) \rangle = e^{-v_p^0 t}, \quad v_p^0 = \frac{p^2}{\tau_R}, \quad \tau_R = \frac{\zeta N^2 l^2}{3\pi^2 kT} = \frac{N^2}{W\pi^2}, \quad \frac{1}{6} \langle [x_0(t) - x_0(0)]^2 \rangle = D_R t = \frac{kT}{N\zeta} t, \quad (2)$$

where ζ is the monomeric friction coefficient, D_R the Rouse diffusion coefficient, and W the Rouse rate. Topological constraints will change the relaxation behavior for each mode differently but not their spatial extension—the chains remain Gaussian.

The contribution of the different normal modes to the dynamic structure factor depends strongly on the momentum transfer Q . Since $S(Q,t)$ does not simply decompose into a sum of contributions from the different modes, we define contribution factors

$$R_p(Q) = \sum_{m,n} \exp \left\{ -\frac{1}{6} Q^2 l^2 |m-n| - \frac{4R_g^2 Q^2}{\pi^2} \frac{1}{p^2} \cos \left[\frac{p\pi m}{N} \right] \cos \left[\frac{p\pi n}{N} \right] \right\} / S(Q,t=0). \quad (3)$$

They describe to what extent a mode “ p ” may relax $S(Q,t)$ in the limit of long times ($t \rightarrow \infty$) and under the premise that all other modes are not active [$\{1 - \langle x_j(t)x_j(0) \rangle\} = 0$ for $j \neq p$]. Figure 2 displays $R_p(Q)$ for the two low M_w polymers considered in Fig. 1. The vertical lines indicate the experimental Q values. Viewing the contribution factors for the PE 2000 sample we realize that at the two smallest experimental Q values ba-

sically only translational diffusion plays a role [it appears as a front factor in Eq. (1)]. At $Q = 0.077 \text{ \AA}^{-1}$ the first relaxation mode comes into play. For $Q = 0.115 \text{ \AA}^{-1}$ we get a significant contribution from the second mode. Finally, at $Q = 0.155 \text{ \AA}^{-1}$ higher modes contribute. This Q -dependent onset of different normal modes in the dynamic structure factor offers the opportunity to determine

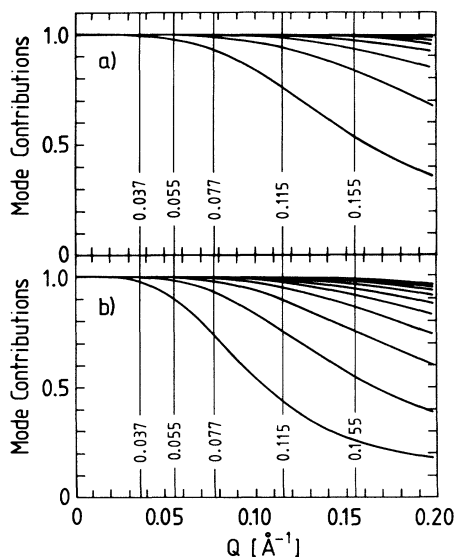


FIG. 2. Contribution factors $R_p(Q)$ of the different modes to $S(Q,t)/S(Q,0)$ (see text) for the (a) $M_w=2.0 \times 10^3$ and (b) $M_w=4.8 \times 10^3$ sample. The experimental Q values are indicated by vertical lines. The Q -dependent decay of $R_p(Q)$ decreases with increasing mode number. Thus, the strongest decay relates to the first mode and so on.

separately the relaxation behavior of these modes.

In a zero order approximation we fitted the spectra in terms of the Rouse model using Eqs. (1) and (2). This approach fails, rendering strongly molecular weight dependent Rouse rates and wrong spectral shapes. In a first iteration we kept the exponential decay of the normal modes but assigned mode dependent relaxation rates:

$$\tilde{\nu}_p = (\pi^2 p^2 / N^2) W_p. \quad (4)$$

Explicitly the fitting procedure included independent relaxation rates for the first three modes, another rate for all higher modes, and the translational diffusion coefficient [11]. The solid lines in Fig. 1 display the resulting theoretical spectra. Table I presents the results.

Figure 3 displays the experimentally obtained rates W_p as a function of mode number for the different molecular weights. For the sample with the lowest M_w the rates for all modes come out essentially identical. On the time scale of the experiment this chain undergoes Rouse dynamics though the diffusion coefficient is already reduced compared to the theoretical value for a Rouse chain,

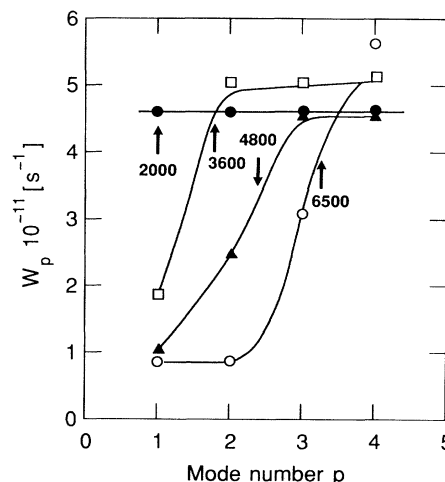


FIG. 3. Relaxation rates W_p for the first four modes for chains of different molecular weight as a function of the mode number p . For each molecular weight the arrows indicate the condition $p=N/N_e$ (error bars, see Table I). The solid lines are guides to the eye.

$$D_R = \frac{kT}{N\rho} = \frac{Wl^2}{3N} = 14.3 \times 10^{-7} \text{ cm}^2/\text{s}.$$

Starting with the PE 3600 sample the rates for the lower modes are systematically reduced. While for the PE 3600 sample this relates only to the first mode, for large molecular weights higher modes are also affected. As can be seen from a detailed comparison of the predicted curves to the experimental data, the agreement is not perfect. In particular at short times and for higher molecular weights discrepancies occur. This suggests that the approach of an exponential correlation function for the normal modes may still be too rough. On the other hand, the mode analysis clearly shows an important and seemingly essential feature of the crossover to entanglement controlled dynamics. The long wavelength relaxation modes are increasingly slowed down while the shorter wavelength modes are not affected.

This observation may be quantified in terms of the entanglement length d , which for long PEB-2 chains has been determined by NSE to be $d=43.5 \text{ \AA}$ [4] corresponding to $M_e=2.0 \times 10^3$ or $N_e=M_0/m_0=137$ (m_0 : molecular weight/main chain bond). The spatial extension of a mode p along the chain covers $n_p=N/p$ bonds. We now may ask how the slowing down of the first modes

TABLE I. Results of the mode analysis and comparison to the macroscopic diffusion (D_{NMR}) and viscosity (η) data by Pearson *et al.* [12].

Sample	$W_p \times 10^{-11}$				$D_n \times 10^7$ (cm^2/s)	$D_{\text{NMR}} \times 10^7$ (cm^2/s)	η (P)	η_{cal} (P)
	$p=1$	$p=2$	$p=3$	$p>3$				
PE 2000	4.6 ± 0.4	4.6 ± 0.4	4.6 ± 0.4	4.6 ± 1.0	8.6 ± 0.15	10.3	0.08	0.11 ± 0.012
PE 3600	1.9 ± 0.2	5.0 ± 0.5	5.1 ± 0.5	5.1 ± 0.6	3.1 ± 0.16	3.6	0.35	0.38 ± 0.04
PE 4800	1.0 ± 0.2	2.4 ± 0.4	4.1 ± 0.5	4.5 ± 1.0	1.9 ± 0.19	1.6	0.96	0.9 ± 0.18
PE 6500	0.87 ± 0.16	0.87 ± 0.16	3.1 ± 0.4	5.6 ± 0.7	1.6 ± 0.18	0.57	1.84	1.64 ± 0.3

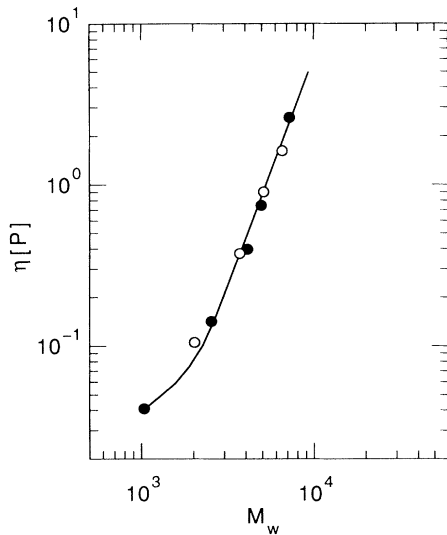


FIG. 4. Rescaled and calculated viscosities for PEB-2 melts at 509 K as a function of molecular weight (●, experimental results [12]; ○, calculated viscosities on the basis of the mode analysis). The solid line serves as a guide to the eye.

may be related to N_e . In Fig. 3 the arrows $p = N/N_e$ for different chains are indicated. Obviously modes with $p \geq N/N_e$ are not modified while modes with $p < N/N_e$ are strongly suppressed.

Thus, the NSE experiment reveals some important insight into the process of entanglement formation: (i) The internal dynamics of a short chain with $N \sim N_e$ is described well by the Rouse model though some reduction of the diffusion coefficient is already apparent. (ii) If the chain length is increased beyond N_e internal modes reflecting intrachain distances smaller than N_e persist, while relaxation modes corresponding to longer distances relax on a much longer time scale. (iii) The transition appears to be sharp and is governed by M_e rather than by $M_c \approx 2.5M_e$, the critical molecular weight for the viscosity crossover. Thus, with respect to the internal modes of a chain the formation of entanglement constraints expresses itself in a strong slowing down of large-scale modes with $n_p > N_e$.

In the final part of this paper we compare our results on the dynamic structure factor to recent macroscopic diffusion and viscosity measurements on PEB-2 chains with different M_w by Pearson *et al.* [12], which have been performed at $T = 175^\circ\text{C}$. In order to relate to our experiments carried out at $T = 236^\circ\text{C}$ we rely on extensive temperature and M_w dependent experiments on polyethylene again by Pearson *et al.* [13], who explored the temperature shift factors for the monomeric friction coefficients over a large range of M_w and T . As may be seen from Table I with the exception of the PE 6500 sample we found good agreement between the rescaled pulse field gradient NMR diffusion data of Pearson *et al.* [12] and our NSE results obtained at a much shorter length and time scale. The discrepancy at $M_w = 6.5 \times 10^3$ may

be related to the shortness of our time scale ($t_{\max} < 2 \times 10^{-8}$ s). At times much shorter than the relaxation time of the slowest internal mode ($\tau_1 = 2.3 \times 10^{-7}$ s) the center of mass motion may not yet have reached the asymptotic diffusion value [2].

In order to compare with viscosity results we resort to the general relation between viscosity and dynamic modulus $G(t)$ and internal relaxation times τ_i [14],

$$\eta = \int_0^\infty dt G(t) = \frac{\rho N_A}{M} \frac{kT}{2} \sum_i \tau_i, \quad (5)$$

where ρ is the polymer density and N_A the Avogadro number. Again assuming the above mentioned $\rho(M, T)$ relationship we rescaled the viscosity results to 509 K and in Table I compare them with a calculation on the basis of Eq. (5) using $\rho(509 \text{ K}) = 0.733 \text{ g/cm}^3$ and the rates of Table I converted to relaxation times following Eq. (4). As can be seen from Table I and Fig. 4 the agreement between the measured viscosities and the calculation on the basis of a mode analysis of the dynamic structure factor is excellent, demonstrating the internal consistency of the results.

We would like to thank Professor E. Donth for a stimulating discussion and express our gratitude to Professor Pearson for communicating his viscosity and diffusion results prior to publication. Furthermore, we are grateful to the Laboratoire Léon Brillouin for providing the beam time.

- [1] J. D. Ferry, *Viscoelastic Properties of Polymers* (Wiley, New York, 1980).
- [2] M. Doi and S. F. Edwards, *The Theory of Polymer Dynamics* (Clarendon, Oxford, 1986).
- [3] D. Richter, B. Farago, L. J. Fetters, J. S. Huang, B. Ewen, and C. Lartigue, *Phys. Rev. Lett.* **64**, 1389 (1991).
- [4] D. Richter, R. Butera, L. J. Fetters, J. S. Huang, B. Farago, and B. Ewen, *Macromolecules* **25**, 6156 (1992).
- [5] See, e.g., F. Mezei, in *Neutron Spin Echo*, Lecture Notes in Physics Vol. 128, edited by F. Mezei (Springer-Verlag, Berlin, 1980).
- [6] P. E. Rouse, *J. Chem. Phys.* **21**, 1273 (1953).
- [7] P. G. de Gennes, *Physics* (Long Island City, N.Y.) **37**, 3 (1967).
- [8] G. J. Ronca, *J. Chem. Phys.* **79**, 79 (1983).
- [9] Theoretically for short chains deviations from the Gaussian chain character have been predicted [J. D. McCoy, K. G. Honnel, J. G. Curro, K. S. Schweizer, and J. D. Honeycutt, *Macromolecules* **25**, 4905 (1992)]. Such deviations become important for $(QL)^2 > 0.15$, where $L = 1.54 \text{ \AA}$ is the bond length. In the Q range of the experiment $(QL)^2$ at maximum amounted to 0.05.
- [10] A. T. Boothroyd, A.R. Rennie, and C. B. Boothroyd, *Europhys. Lett.* **15**, 715 (1991).
- [11] In the fitting routine we imposed the bias that relaxation rates should not decrease with increasing mode number.
- [12] D. S. Pearson, L. J. Fetters, W. W. Graessley, G. Ver Strate, and E. von Merwall (to be published).
- [13] D. S. Pearson, G. Ver Strate, E. van Merwall, and F. C. Schilling, *Macromolecules* **20**, 1133 (1987).
- [14] W. W. Graessley, *Adv. Polymer Science* **16**, 1 (1974).